Research Article

Biwei Luo, Pengfei Li, Yan Li, Jun Ji, Dongsheng He, Qifeng Tian*, and Yichang Chen*

Feasibility of fly ash as fluxing agent in mid- and low-grade phosphate rock carbothermal reduction and its reaction kinetics

https://doi.org/10.1515/gps-2021-0008
received September 23, 2020; accepted December 27, 2020

Abstract: The feasibility of industrial waste fly ash as an alternative fluxing agent for silica in carbothermal reduction of medium-low-grade phosphate ore was studied in this paper. With a series of single-factor experiments, the reduction rate of phosphate rock under different reaction temperature, reaction time, particle size, carbon excess coefficient, and silicon–calcium molar ratio was investigated with silica and fly ash as fluxing agents. Higher reduction rates were obtained with fly ash fluxing instead of silica. The optimal conditions were derived as: reaction temperature 1,300°C, reaction time 75 min, particle size 48–75 μm, carbon excess coefficient 1.2, and silicon–calcium molar ratio 1.2. The optimized process condition was verified with other two different phosphate rocks and it was proved universally. The apparent kinetics analyses demonstrated that the activation energy of fly ash fluxing is reduced by 31.57 kJ/mol as compared with that of silica. The mechanism of better fluxing effect by fly ash may be ascribed to the fact that the products formed within fly ash increase the amount of liquid phase in the reaction system and promote reduction reaction. Preliminary feasibility about the recycling of industrial waste fly ash in thermal phosphoric acid industry was elucidated in the paper.

Keywords: phosphate rock, fly ash, carbothermal reduction, apparent kinetics

*** Corresponding author: Qifeng Tian,** School of Chemical Engineering and Pharmacy, Wuhan Institute of Technology, Wuhan 430205, China; Key Laboratory of Green Chemical Process of Ministry of Education and Key Laboratory of Novel Reactor and Green Chemical Technology of Hubei Province, Wuhan Institute of Technology, Wuhan 430205, China; National Engineering Research Centre of Phosphate Resource Development and Utilization and Engineering Research Centre of Phosphate Resource Development and Utilization, Ministry of Education, Wuhan 430074, China, e-mail: qftian@wit.edu.cn
*** Corresponding author: Yichang Chen,** Hubei Research and Design Institute of Chemical Industry, Wuhan 430074, China, e-mail: hb_chem@126.com
Biwei Luo: School of Chemical Engineering and Pharmacy, Wuhan Institute of Technology, Wuhan 430205, China, e-mail: yfnysryg@163.com
Pengfei Li: School of Chemical Engineering and Pharmacy, Wuhan Institute of Technology, Wuhan 430205, China, e-mail: ffsrlin@163.com
Yan Li: School of Chemical Engineering and Pharmacy, Wuhan Institute of Technology, Wuhan 430205, China, e-mail: li_yanyan@163.com
Jun Ji: School of Chemical Engineering and Pharmacy, Wuhan Institute of Technology, Wuhan 430205, China; Key Laboratory of Green Chemical Process of Ministry of Education and Key Laboratory of Novel Reactor and Green Chemical Technology of Hubei Province, Wuhan Institute of Technology, Wuhan 430205, China, e-mail: sand_wing@163.com
Dongsheng He: Key Laboratory of Green Chemical Process of Ministry of Education and Key Laboratory of Novel Reactor and Green Chemical Technology of Hubei Province, Wuhan Institute of Technology, Wuhan 430205, China; Xingfa School of Mining Engineering, Wuhan Institute of Technology, Wuhan 430074, China; National Engineering Research Centre of Phosphate Resource Development and Utilization and Engineering Research Centre of Phosphate Resource Development and Utilization, Ministry of Education, Wuhan 430074, China, e-mail: hds@wit.edu.cn

1 Introduction

Phosphoric acid is an important chemical raw material, and its products are widely used in various fields such as medicine, chemical industry, agriculture, national defense, and so on. At present, there are three main methods for producing phosphoric acid: wet-process phosphoric acid, thermal-process phosphoric acid, and kiln-process phosphoric acid. The wet-process phosphoric acid process requires the use of high-grade phosphate rock, and the subsequent separation process is complicated [1]. Kiln-process phosphoric acid is not yet mature in technology and process and is still under research [2]. Mid- and low-grade phosphate rock can be directly used in the thermal-process phosphoric acid, but there is a problem of high energy consumption [3,4]. For

most of the Chinese mid- and low-grade phosphate mines, resource utilization rate is not high. The effective use of mid- and low-grade phosphate rock resources is a necessary way to achieve sustainable development of Chinese phosphorus chemical industry [5]. Therefore, solving the problem of high energy consumption in the thermal phosphoric acid process and making full use of low- and medium-grade phosphate are important to promote the sustainable development of the phosphorous chemical industry.

In order to optimize thermal-process phosphoric acid and achieve the goal of energy saving and consumption reduction, many methods including adding flux or inorganic salts to the phosphate carbothermal reduction system have been reported in the literature. Kaia et al. [6] found in their research work that silica is more effective as an additive than Al_2O_3 and is more conducive to the reaction. Cheng et al. [7] studied the reaction mechanism of phosphate rock with SiO_2, Al_2O_3, and Fe_2O_3 in the case of graphite as a reducing agent and found that SiO_2 and Al_2O_3 are beneficial to the carbothermal reduction reaction of phosphate rock. Cao et al. [8] found that adding a certain amount of alkali metal carbonate to the phosphorite carbothermal reduction reaction system can enhance the activity of carbon, but does not change the reaction paths. Yang et al. [9] reported that the reduction rate and reaction rate of phosphate rock with 5% Al_2O_3 reaction system were higher than those without additives. Hu et al. [10] investigated the influence of inorganic additives (Li_2CO_3, Na_2CO_3, KCl) on the reduction rate of phosphate rock. A comprehensive analysis showed that the promotion effect of three inorganic additives on the carbothermal reduction of phosphate rock was Na_2CO_3 > KCl > Li_2CO_3. Tang et al. [11] studied the effects of SiO_2, Al_2O_3, and MgO fluxes on the melting characteristics of phosphate rock. Their results showed that the addition of the three fluxes can improve the melting characteristics of the material and reduce the melting temperature. The melting point of SiO_2 is lower than the other two fluxes. Chen et al. [12] discussed the effects of four fluxes (silica, potash feldspar, potash shale, nepheline) on the carbothermal reduction of phosphate rock. Finally, the optimal process conditions of the carbothermal reduction reaction of phosphate rock were determined as follows: reaction temperature 1,400°C, time 40 min, acidity value 1.02, and anthracite excess coefficient 1.5. The carbothermal reduction reaction mechanism of silica and potash feldspar fluxing phosphate rock was revealed by Xia et al. [13,14]. The results showed that the reaction temperature can be reduced by potash feldspar fluxing. The activation energy during melting is 3.2 kJ/mol lower than that of silica fluxing. ADF and ADC were used as fluxes for coal melting by Sun et al. [15]. Their results indicated that fluxing minerals can be easily formed with hematite, iron spinel, and coal, thereby reducing coal melting temperature. Jin et al. [16] worked on the effects of the reduction rate of phosphate rock by adding CaO, SiO_2, Al_2O_3, and MgO to the reaction system at the same time. They claimed that the reduction rate of phosphate rock can be increased from 60% to 90%. It is very important that the carbon materials affect the process of phosphate ore, especially the graphitizing extents of carbon fiber increase with the temperature of carbonization. For example, petroleum coke underwent graphitizing more easily than coal as charging temperature increased [17].

The silicon industry is an energy-intensive industry with high energy operating costs and is currently facing new challenges to improve sustainability and become more competitive [18,19]. Fly ash is a kind of industrial waste after coal combustion. It is composed of fine ash collected from flue gas after coal combustion and boiler bottom slag. It is mainly composed of silica and alumina, and a small amount of metal oxides [20]. According to speculation, Chinese total fly ash accumulation will reach about 3 billion tons by 2020 [21]. The accumulation of fly ash will not only pollute the surrounding environment, but also occupy a lot of land resources. Therefore, the purpose of this paper is to use industrial waste fly ash as a flux to improve its economic value and reduce environmental pollution. The fluxing effects of silica and fly ash was compared on the reduction rate of phosphorite carbothermal reduction process. The apparent kinetics analyses of carbothermal reduction process by silica and fly ash are expected to provide theoretical basis for fly ash to be used in thermal phosphoric acid industry.

2 Materials and methods

The phosphate rock used in the experiments was from Mabian (Sichuan Province) and Huangmailing, Yichang

Table 1: Main chemical composition of phosphate rock % (wt)

Source of phosphate rock	P_2O_5	CaO	SiO_2	MgO	Fe_2O_3	Al_2O_3	F
Mabian (Sichuan)	24.9	52.18	9.4	6.64	1.52	1.13	2.52
Huangmailing (Hubei)	18.66	35.48	27.02	3.04	2.17	6.79	1.28
Yichang (Hubei)	19.58	42.23	25.33	7.17	1.45	1.30	1.45

Table 2: Main chemical composition of fly ash % (wt)

Ingredient	P_2O_5	SiO_2	Al_2O_3	CaO
Content	0.14	64.27	24.58	11.01

Table 3: Industrial analysis of reducing agent coke % (wt)

Ingredient	Fixed carbon	Ash	Volatile matter	Moisture
Content	82.03	9.27	4.15	4.55

(Hubei Province), respectively. The main components of phosphate rock were measured by X-ray fluorescence spectrometer and the results are shown in Table 1. The main components of fly ash are demonstrated in Table 2. Silica is the analytical reagent of Sinopharm, and industrial analysis of reducing agent coke is shown in Table 3.

X-ray diffraction (XRD) patterns were performed on a Bruker D8 diffractometer (Germany), using Cu Kα radiation (40 kV, 40 mA). The XRD pattern of the three types phosphate rock in Figure 1 showed that the main components of three types of phosphate rock are $Ca_5(PO_4)_3F$, SiO_2, $CaMg(CO_3)_2$, $KAlSi_3O_8$, etc. There is not much difference in the composition among the three phosphate rocks.

Surface morphology of the catalysts was recorded on a scanning electron microscopy (SEM, JEOL, Japan). The SEM images of the three types of phosphate rock in Figure 2 showed that the phosphate rocks from Mabian and Yichang hold nonuniform particle size distribution, while the phosphate rock from Huangmailing holds more powder and its particles are distributed more evenly than the other two types of phosphate ores.

The materials mixed evenly according to a certain ratio are compressed into a number of Φ 15 mm × 3 mm flakes with a powder tablet press under a pressure of 10 MPa, and 5–6 g flake samples are taken and dried in an oven at 80°C. The dried samples are weighted and placed in a graphite crucible and heated in a high-temperature electric furnace with a preset heating program under high-purity nitrogen flow at a flow rate of 80 mL/min for 30 min to exhaust the air in the furnace. The carbothermal reduction of phosphate rock is conducted under the protection of high-purity nitrogen. The temperature is increased to a specified temperature at a rate of 5°C/min and it kept at a constant temperature for a period of time. During the cooling process, the high-purity nitrogen is still kept in the process and cooling rate is 5°C/min. After the furnace body is cooled to room temperature, the graphite crucible with slag is taken out and weighed. The slag is ground into a powder in a mortar, which is reserved for further analyses.

The content of P_2O_5 in the residue was analyzed by gravimetric method with quinoline phosphomolybdate as agent. The phosphorus rock reduction rate (X) was calculated according to Eq. 1:

$$X = \frac{M - M_1}{M} \times 100\% \quad (1)$$

where M is the mass of P_2O_5 in the samples before the reaction, M_1 is the mass of P_2O_5 in the slags after the reaction.

Reaction temperature (A), reaction time (B), phosphorus rock particle size (C), coke excess coefficient (CEC, D), and molar ratio of silicon–calcium (E) are the factors and phosphorus reduction rate (X) is the response value in the paper.

3 Results and discussion

3.1 Single-factor experiments investigation

The results of single-factor experiments investigation are displayed in Figure 3. The results in Figure 3a showed that the reduction rate increases with reaction temperature. Temperature has a very large effect on the reaction because the carbothermal reduction reaction of phosphate rock is a strong endothermic reaction. With the increase of the reaction temperature, the reduction rate of phosphate rock is gradually increased when the two fluxes are added. From the figure, one can see that the reduction rate of phosphate rock with fly ash as flux is

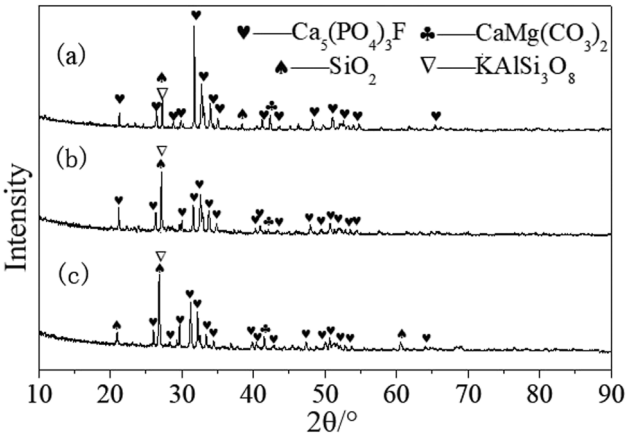

Figure 1: XRD pattern of three types phosphate rock: (a) Mabian, (b) Huangmailing, and (c) Yichang.

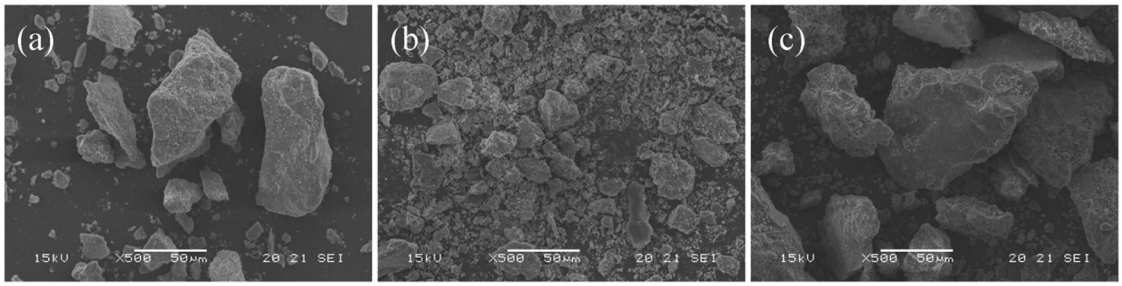

Figure 2: SEM images of three types phosphate rock: (a) Mabian, (b) Huangmailing, and (c) Yichang.

higher than that of SiO_2. Between 1,150°C and 1,300°C, the reduction rate of phosphate rock grows rapidly with the increase of temperature. At temperatures above 1,300°C, the reduction rate of phosphate rock becomes stable. In the low temperature stage, since the carbothermal reduction reaction of phosphate rock is a solid–solid reaction and the mass and heat transfer is limited by solid-phase diffusion, it leads to the low reduction rate at this stage. As the temperature rises, molten state is formed in the reaction system, which ameliorates the diffusion and accelerates mass transfer. With the temperature increasing further, the amount of liquid phase grows, and the viscosity of the solution is reduced, which promotes reaction and improves the reduction rate [22]. As the temperature was increased from 1,300°C to 1,350°C, the reduction rate of phosphate rock under both fluxes was enhanced by less than 2%. Because most of the reactants have already participated in the phosphorite reduction reaction at this time, the formation of new substances and the consumption of raw materials made the contact area between the reactants reduced, and thus the reduction rate of phosphate rock became stable. If the temperature is raised further, the reduction rate of phosphate rock only increases slightly. However, the energy cost will increase significantly. Therefore, the optimum reaction temperature is 1,300°C.

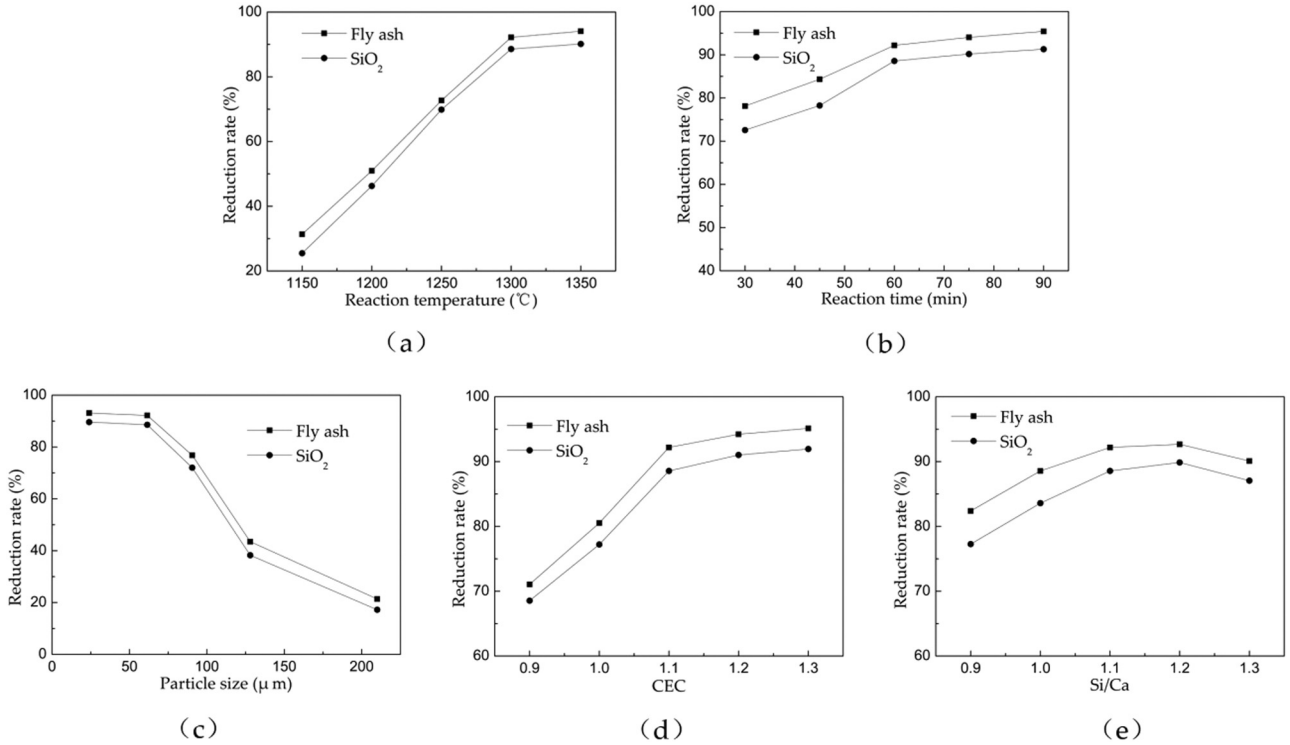

Figure 3: Influence of various factors on reduction rate. (a) Fixed levels A (75 min), C (48~75 μm), D (1.1), E (1.1). (b) Fixed levels A (1,300°C), C (48–75 μm), D (1.1), E (1.1). (c) Fixed levels A (1,300°C), B (75 min), D (1.1), E (1.1). (d) Fixed levels A (1,300°C), B (75 min), C (48–75 μm), E (1.1). (e) Fixed levels A (1,300°C), B (75 min), C (48–75 μm), D (1.1).

As shown in Figure 3b, the reduction rate increases gradually with reaction time. In industrial production, shortening the reaction time is an effective way to reduce energy consumption. Therefore, it is vital to choose an appropriate reaction time [23]. As the reaction time extends, the reduction rate of phosphate rock under both fluxes increases gradually. In the initial stage of the reaction, fluoroapatite diffuses through the solid phase to the surface of the reducing agent at a slow rate. With continuous heating and temperature increasing, liquid phase formed in the system which facilitates mass transfer and increases the reaction rate. As the reaction time increases further, especially as the reaction time increases from 75 to 90 min, the increase of reduction rate becomes even. The effects of temperature on the phosphate rock reduction rate improving are limited in this stage, and energy consumption will cost more than that in lower temperature stage. Therefore, the reaction time was selected as 75 min to study the influence of other factors on the reduction rate of phosphate rock.

The phosphorus rock particle size influences the heat and mass transfer and thereby the reduction rate. Figure 3c showed that as the particle size of phosphate rock decreases, the reduction rate of phosphate rock with both fluxes increases rapidly. For the phosphate rock, particle size is reduced from 150–270 to 48–75 μm, the reduction rate of fly ash fluxing system is increased by 70.82%, while 71.34% for the silica fluxing system. As the particle size of phosphate rock is reduced from 48–75 to 0–48 μm, the changes of reduction rate of phosphate rock with both two fluxes are less than 2%, and the difference in reduction rate is minor to be neglected. It is clearly indicated that the larger particle size leads to the reduced contact area between the reactants and insufficient reaction and lower reduction rate. On another hand, part of the refractory material generated by the reaction encapsulates the ore particles, which hinders the contact between the reactants and prevents the reaction from proceeding fully [24]. For the particle with large size, the heat transfer between the outer layer and the inside of the sample is not timely because of the limited effective contact area between the reactants. Therefore, the reaction is always controlled by solid diffusion in this case. Phosphate rock with small particle size is heated more uniformly, and the contact area between the reactants is larger, which facilitate generating molten liquid phase and increase the driving force of the reaction. Consequently, reducing the particle size of phosphate rock can effectively increase the rate of carbothermal reduction reaction of phosphate rock and increase reaction efficiency. Therefore, 48–75 μm is chosen as the optimum particle size to study the influence of other factors on the reduction rate of phosphate ore.

During the smelting reduction of phosphate rock, coke not only acts as a reducing agent, but also has a conductive effect [25]. Considering the effects of the amount of reduction agent coke on the reduction rate, the relation between different CECs and the reduction rate was demonstrated in Figure 3d, in which the reduction rate increases with CEC. When the carbon excess coefficient is 0.9, the amount of reducing agent is insufficient, resulting in a part of the reactants cannot be reduced and the phosphate rock reduction rate being low. When the carbon excess coefficient is 1.1–1.2, excessive coke will promote unreacted phosphate rock continuing to carry out the reduction reaction to improve the reduction rate. However, as the carbon excess coefficient was increased to 1.3, the reduction rate of the phosphate rock in the two fluxing systems was increased by less than 1%, which denotes the existence of limit for the amount of carbon on the increasing reduction rate of the phosphate rock, which is consistent with the conclusion by Mu et al. [26] that excessive carbon has little effect on the reduction rate. So, the carbon excess coefficient is selected as 1.2.

The effects of molar ratio of silicon–calcium (Si/Ca) on the reduction rate were investigated and the results are shown in Figure 3e. The flux not only participates in the carbothermal reduction reaction of phosphate rock, but also decreases the melting temperature and starting temperature of the reaction. Silica can form calcium silicate with fluorapatite at high temperature, decrease the initial reduction temperature of fluorapatite to promote the reduction of fluorapatite, and increase the reduction rate of apatite. At the same time, silica is an acidic oxide. Excessive silica will increase the viscosity of the material and hinder defluorination. After the reduction degree reaches the peak, as the silica content continues to rise, the reduction degree of fluoroapatite begins to decrease slightly. Without other additives, fluoroapatite will undergo defluorination reaction at 1,174°C to form $Ca_3(PO4)_2$ and CaF_2 and will be reduced by carbon to CaF_2, CaO, and P_2 at 1,439°C. SiO_2 and Al_2O_3 can lower the initial reduction temperature of fluorapatite from 1,439°C to 1,204°C and 1,247°C, respectively [27,28]. Because the addition of flux changes the reduction environment of phosphate rock smelting, the reduction rate of phosphate rock increases faster when the ratio of silicon to calcium is increased from 0.9 to 1.1. The ratio of large silicon to calcium is equivalent to increasing the total surface area of the mixed reactants, which is beneficial to the reduction reaction of phosphate rock and thus improves the reduction rate.

When the silicon-to-calcium ratio is increased from 1.2 to 1.3, the phosphate ore reduction rate actually decreases, indicating that the phosphate concentration in the system will be reduced instead when too much flux is added, which will reduce the driving force of the reaction and phosphorus reduction. Therefore, the ratio of silicon to calcium is determined to be 1.2.

3.2 Verification experiment

Based on the above investigation on the influencing factors of carbothermal reduction reaction of phosphate rock, the optimum conditions of the carbothermal reduction reaction of phosphate rock are: reaction temperature 1,300°C, reaction time 75 min, molar ratio of silicon to calcium 1.2, carbon excess coefficient 1.2, and the particle size is 48–75 μm. At this time, the reduction rate of phosphate rock with fly ash as flux reached 94.21%, while the reduction rate of phosphate rock with silica as flux reached 91.03%. Therefore, fly ash can be used as substitution for SiO_2 as fluxing agent for carbothermal reduction reaction of phosphate rock. Furthermore, the reduction rate of phosphorus with fly ash as fluxing agent is slightly higher than that with SiO_2. Fly ash, as a kind of solid waste, can be used as fluxing agent in the thermal-process phosphoric acid process. Our results open a new way to recycle fly ash in green processing and sustainable development.

In order to verify whether the optimum conditions are universal, experiments were carried out under the above optimum conditions with phosphate mines from Huangmailing and Yichang, Hubei Province, respectively. The results are shown in Figure 4. It can be seen from Figure 4 that the reduction rates of the other two types of phosphate ores under the optimum condition are close to or higher than those of the Mabian phosphate ore, which were used in the single-factor experiments. The results of Figure 4 indicated that the optimum conditions hold certain universality. Under the optimum conditions, the fluxing effect of fly ash is better than that of silica. Since fly ash is industrial waste, using fly ash as a flux can save resources and protect environment.

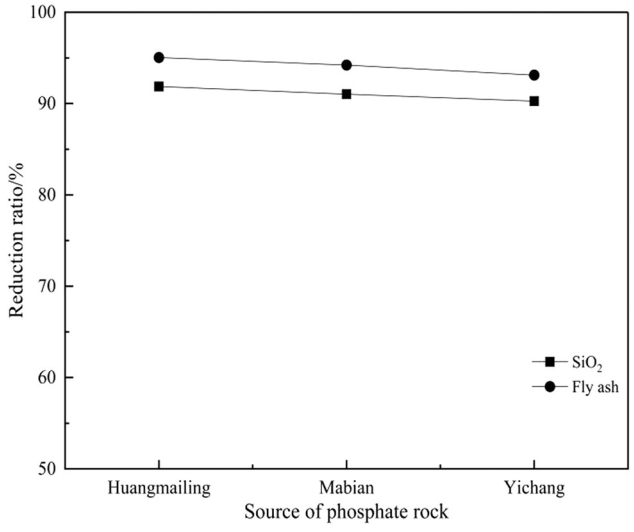

Figure 4: Reduction rate of different phosphate rock under optimized conditions.

3.3 Kinetic analysis of different flux systems

In order to further study the effects of fly ash and silica on the carbothermal reduction of phosphate rock, apparent kinetic analysis experiments were carried out on the two fluxing systems of fly ash and silica, respectively. Under the conditions of the above optimum conditions, the relationship between the reduction rate of phosphate rock at 1,200°C, 1,250°C, 1,300°C, and 1,350°C and holding time was investigated. The results are shown in Figure 5.

The differential method is used to calculate the reaction order. According to the principle of reaction kinetics, the differential form of the phosphate ore thermal reduction reaction rate equation is shown in Eq. 2:

$$r_A = -\frac{dC_A}{dt} \tag{2}$$

The dynamic equation is shown in Eq. 3:

$$r_A = kC_A^n \tag{3}$$

$$C_A = 1 - X \tag{4}$$

Substituting Eq. 4 into Eq. 2 and Eq. 3, Eq. 5 is:

$$r_A = \frac{dX}{dt} = k(1 - X)^n \tag{5}$$

Taking the logarithms on both sides of Eq. 5, one can get:

$$\log\ r_A = \log\ k + n\log(1 - X) \tag{6}$$

In Eq. 2–6, r_A is reaction rate, n is reaction order, t is time, k is rate constant, C_A is the ratio of the mass of phosphorus in the slag to the amount of phosphorus in the mixture in the reactant, and X is the reduction rate.

The relationship between the reduction rate of phosphate rock in different fluxing systems with time is shown in Figure 5. The slope of the curve is obtained at the

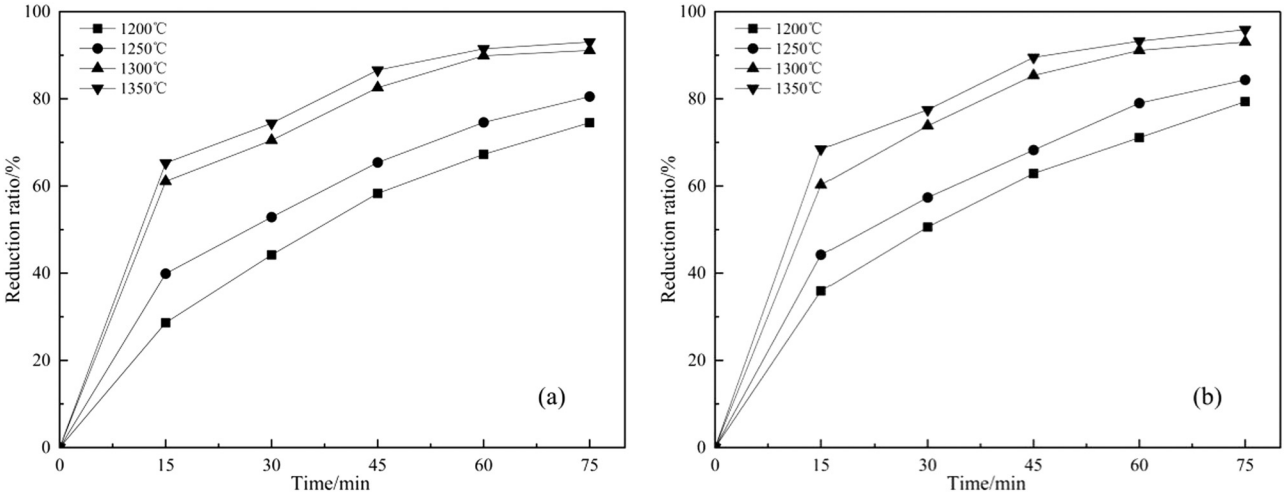

Figure 5: Relationship between the reduction rate containing SiO_2 (a) and fly ash (b) at different reaction time and temperatures.

corresponding reduction rate. This slope dX/dt is the reaction rate as defined in Eq. 5. The relationship between the reaction rate and the time is shown in Figure 6.

It can be seen from Figure 6 that the reaction rate of the two fluxing systems at four temperatures is the largest within 0–15 min, which implies the beginning of the reaction is a process of rapid heat absorption. The driving force of the reaction and the reaction rate is the largest at this stage. As the reaction proceeds, the reactants are continuously consumed and the products are continuously accumulated, which decreases the reaction driving force and slows down the reaction rate. This phenomenon is more obvious at higher temperatures.

It can be seen from Eq. 6 that with $\log(1 - X)$ as the abscissa and $\log r_A$ as the ordinate, a straight line could be fitted, as shown in Figure 7. The slope of the fitted line is the reaction order n, and the intercept is the logarithm of the reaction rate constant k. The reaction order n and reaction rate constants k of the two fluxing systems at different temperatures were calculated and the results were listed in Table 4.

It can be seen from Table 4 that all kinetic equations are fitted as linear. The reaction order of the carbothermal reduction reaction of silica and fly ash fluxing phosphate rock is not a definite value, and it changes with temperature. One reason may be the carbothermal reduction reaction of fluoroapatite is a multistep complex reaction. Different chemical reactions proceed to different degrees at different temperatures. Therefore, as the temperature changes, the reaction order varies. Second, the reaction starts from the solid–solid phase. As the temperature

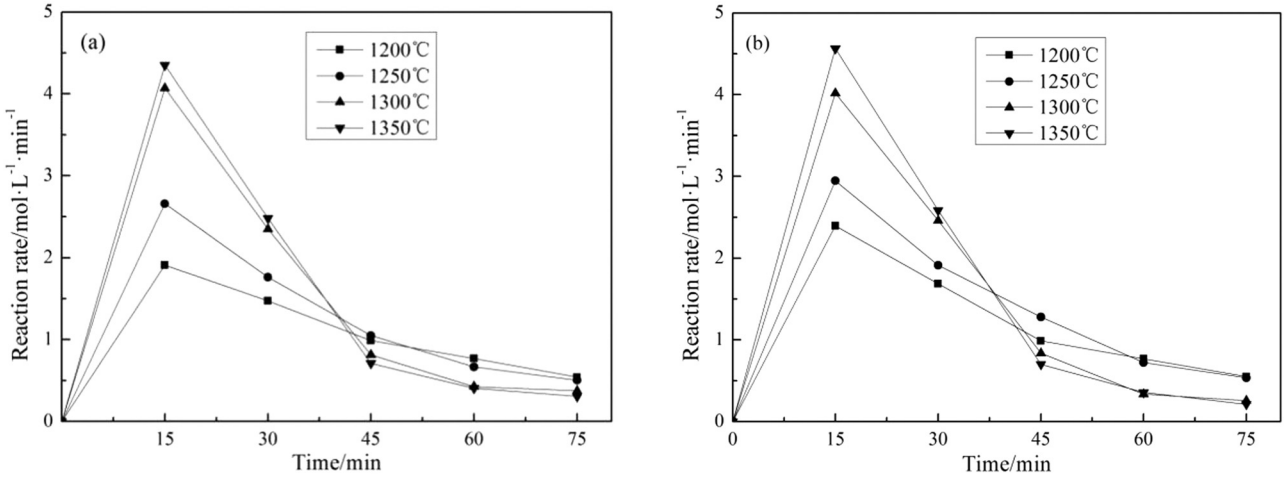

Figure 6: Relationship between the reaction rate containing SiO_2 (a) and fly ash (b) at different reaction time and temperatures.

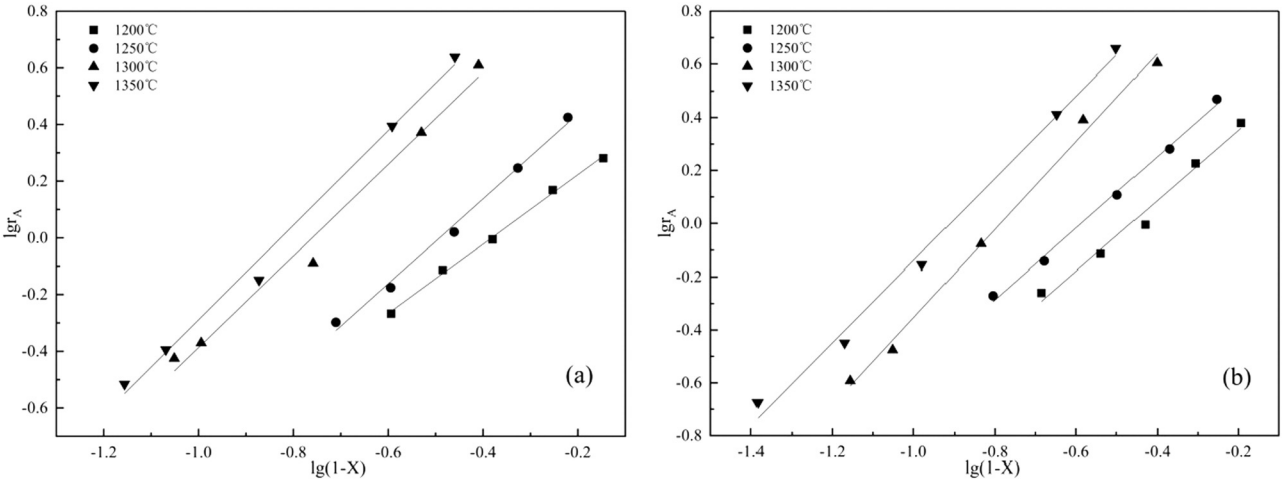

Figure 7: Fitting plots of log r_A and log(1 – X) at different temperatures: (a) SiO_2, (b) fly ash.

increases, the reaction gradually transitions to the solid–liquid phase from the perspective of diffusion, which leads to the reaction order varying with temperature [29]. The reaction order reflects the influence of the material concentration on the reaction rate. The larger the reaction order, the greater the effect of the material concentration on the reaction rate. Therefore, the grade of phosphate rock, that is the concentration of P_2O_5, has a more significant effect on the carbothermal reduction reaction process of phosphate rock at high temperature than low temperature. At the same temperature, the reaction rate constant k of the fly ash fluxing system is larger than that of the silica. This means that under the same reaction conditions, the rate of carbothermal reduction of phosphate rock with fly ash as flux is faster than that of silica. It is believed that the components Al_2O_3 and CaO in fly ash promote carbothermal reduction of phosphate rock [9]. Products such as Al_2SiO_5, $AlPO_4$, and $CaAl_2Si_2O_8$ appearing in the reaction system containing Al_2O_3 increase the liquid phase of the reaction system and promote the carbothermal reduction reaction. According to Liu [30], products such as Al_2SiO_5, $AlPO_4$, and $CaAl_2Si_2O_8$ formed from Al_2O_3 and CaO increase the amount of liquid phase in the reaction system and promote the carbothermal reduction reaction. Activation energy is an important parameter in the kinetics study. The value of activation energy can not only reflect the sensitivity of the reaction rate to temperature, but also the difficulty of the reaction. According to Arrhenius Eq. 7, combined with the data in Table 4, a linear fitting between ln k and 1/T was obtained, as shown in Figure 8. From the slope of the fitted line, the activation energy value of carbothermal reduction reaction can be derived.

$$\ln k = \ln A - \frac{E_a}{RT} \tag{7}$$

where E_a is the reaction activation energy, kJ/mol; A is the pro-factor, min^{-1}; R is the ideal gas constant, 8.314 J/(mol K); T is the temperature, K. The fitted activation energies of carbothermal reduction reaction with fly ash and silica are 264.16 and 295.72 kJ/mol, respectively. The activation energy of carbothermal reduction reaction

Table 4: Linear fit results for different fluxing systems

Fluxing system	Temperature (°C)	Fitted equation	R^2	Reaction order n	Reaction rate constant k
SiO_2	1,200	$y = 1.22X + 0.47$	0.99	1.22	2.93
	1,250	$y = 1.50X + 0.74$	0.99	1.50	5.45
	1,300	$y = 1.62X + 1.23$	0.98	1.62	16.92
	1,350	$y = 1.67X + 1.38$	0.99	1.67	23.92
Fly ash	1,200	$y = 1.33X + 0.62$	0.97	1.33	4.14
	1,250	$y = 1.35X + 0.79$	0.99	1.35	6.18
	1,300	$y = 1.66X + 1.30$	0.99	1.66	20.08
	1,350	$y = 1.55X + 1.41$	0.99	1.55	25.55

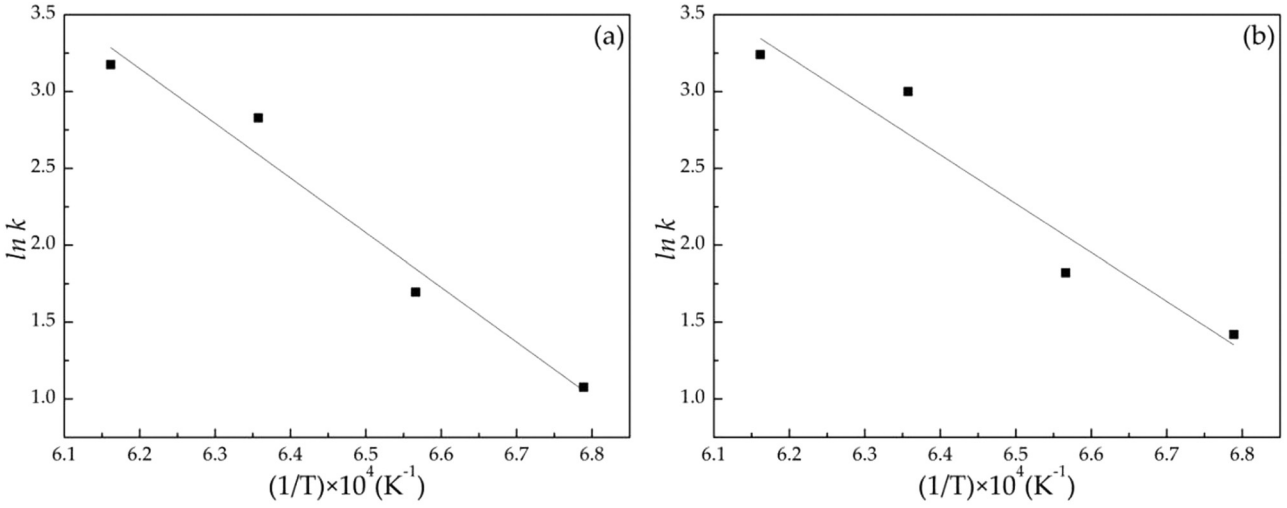

Figure 8: Fitting plots of ln k and $1/T$ at different temperatures: (a) SiO_2, (b) fly ash.

is decreased by using fly ash as fluxing agent instead of silica. The existence of Al_2O_3 and CaO in fly ash is probably beneficial to carbothermal reduction reaction of phosphate rock.

3.4 Analysis of the carbothermal reduction between SiO_2 and fly ash

In order to elucidate the mechanism of enhancement effects of fly ash fluxing, the slags of 48–75 μm phosphate particle after reaction at 1,300°C and 75 min with CEC 1.2 and Si/Ca 1.2 were characterized by optical micro-photographing, XRD and SEM, respectively. Figure 9 showed the optical images of residues taken out after reaction. It can be seen from the figure that the shape of the slag obtained from the silica system showed little change from the original sample, while the residue from the fly ash system showed obvious phenomenon of melting, which indicated that the reaction in the fly ash system proceeded more thoroughly than that of silica system. The difference of optical images between two fluxing system implied that the reduction rate of fly ash fluxing is higher than that of silica fluxing.

The XRD patterns of reduction products were shown in Figure 10. One can see that $Ca_5(PO_4)_3F$, SiO_2, $CaSiO_3$, and $CaMgSi_2O_6$ appeared in the reaction both for two systems. $CaMgSi_2O_6$ may be derived from the reaction of $CaMg(CO_3)_2$ in phosphate rock, while the produced Ca_3SiO_5 in the fly ash system indicated that the fluxing effect is stronger and it can promote the reduction of more calcium phosphate to produce CaO. It provided an opportunity to further react with $CaSiO_3$ to form Ca_3SiO_5, which indicated that fly ash is more conducive than SiO_2 as a flux to promote carbothermal reduction of phosphate rock [31]. In addition, products such as Al_2SiO_5, $AlPO_4$, and $CaAl_2Si_2O_8$ were found in the fly ash fluxing system and are in agreement with the report by Liu [30]. According to the results of XRD, possible reaction mechanisms were proposed as in the following.

For fly ash fluxing system:

$$4Ca_5(PO_4)_3F + 30C + 21SiO_2 \rightarrow 6P_2(g) + 30CO(g) + 20CaSiO_3 + SiF_4(g) \quad (8)$$

$$4Ca_5(PO_4)_3F + 3SiO_2 \rightarrow 6Ca_3(PO_4)_2 + 2CaSiO_3 + SiF_4(g) \quad (9)$$

$$Ca_3(PO_4)_2 + 5C \rightarrow 3CaO + 5CO(g) + P_2(g) \quad (10)$$

$$Ca_3(PO_4)_2 + Al_2O_3 \rightarrow AlPO_4 + 3CaO \quad (11)$$

$$CaSiO_3 + 2CaO \rightarrow Ca_2SiO_5 \quad (12)$$

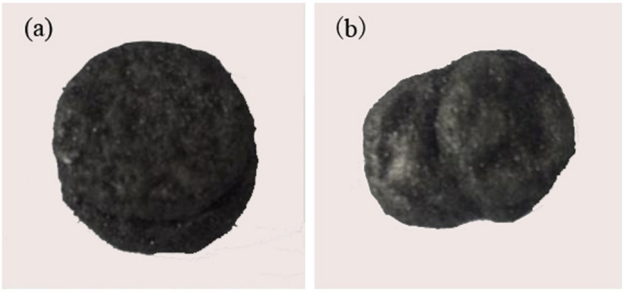

Figure 9: Optical images of residue of SiO_2 system slag (a) and fly ash system slag (b).

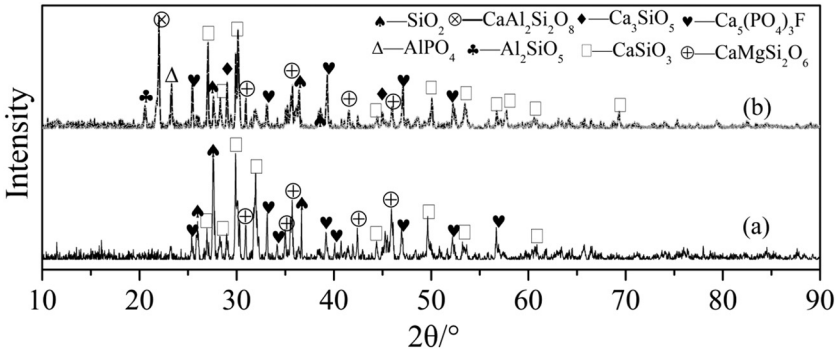

Figure 10: XRD images of SiO_2 system slag (a) and fly ash system slag (b) at 1.300°C.

$$Al_2O_3 + SiO_2 \rightarrow Al_2SiO_5 \quad (13)$$

$$CaO + 2SiO_2 + Al_2O_3 \rightarrow CaAl_2Si_2O_8 \quad (14)$$

$$CaMg(CO_3)_2 + 2SiO_2 \rightarrow CaMgSi_2O_6 + 2CO_2(g) \quad (15)$$

For silica fluxing system:

$$4Ca_5(PO_4)_3F + 30C + 21SiO_2 \rightarrow 6P_2(g) + 30CO(g) + 20CaSiO_3 + SiF_4(g) \quad (16)$$

$$4Ca_5(PO_4)_3F + 3SiO_2 \rightarrow 6Ca_3(PO_4)_2 + 2CaSiO_3 + SiF_4(g) \quad (17)$$

$$Ca_3(PO_4)_2 + 5C \rightarrow 3CaO + 5CO(g) + P_2(g) \quad (18)$$

$$CaMg(CO_3)_2 + 2SiO_2 \rightarrow CaMgSi_2O_6 + 2CO_2(g) \quad (19)$$

The SEM images of slags obtained by reducing the phosphate ore with different fluxing agents are displayed in Figure 11. The surface residue of the sample with SiO_2 fluxing is smooth, as shown in Figure 11a. However, the surface residue from the sample with fly ash fluxing is relatively rougher, as shown in Figure 11b. This may be due to the formation of a large amount of eutectic calcium silicon in the latter [14].

4 Conclusions

In this paper, the carbothermal reduction reaction process of fluxing phosphate rock with two fluxing systems of silica and fly ash was studied. Through single-factor experiments, the carbothermal reduction process of phosphate rock with five factors was investigated. The apparent kinetics study of the two fluxing systems was carried out and the following conclusions were drawn:

(1) When the carbothermal reduction conditions are the same, the reduction rate of fly ash fluxing system is always higher than that of silica. The optimized carbothermal reduction reaction conditions were phosphate particle size 48–75 μm, temperature 1,300°C, time 75 min, carbon excess coefficient 1.2, and silicon–calcium molar ratio 1.2. The optimal conditions were verified by using other phosphate ores with different sources and grades. The results confirmed that the optimal conditions are universal.

(2) For the apparent kinetic study of two fluxing systems, it was found that effect of the grade of phosphate rock on the carbothermal reduction rate is more

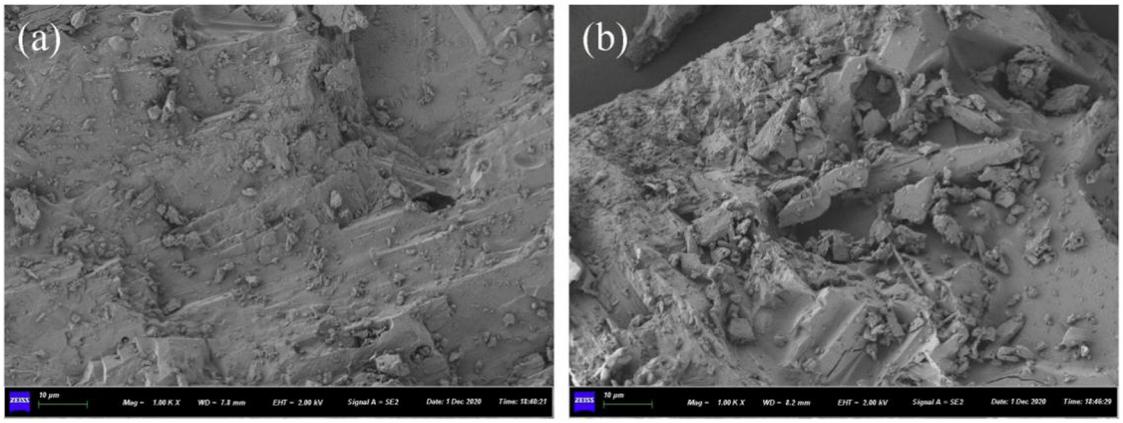

Figure 11: SEM images of SiO_2 system slag (a) and fly ash system slag (b).

significant at high temperature than at low temperature. Under the same reaction conditions, the rate of phosphate rock carbothermal reduction with fly ash as flux is faster than that of silica. Compared with silica, the activation energy of fly ash fluxing system is reduced by 31.56 kJ/mol. Therefore, fly ash is more energy-saving than traditional silica as a flux.

(3) The mechanism of better fluxing effect by fly ash may be ascribed to the products such as Al_2SiO_5, $AlPO_4$, and $CaAl_2Si_2O_8$ formed from the components Al_2O_3 and CaO within fly ash, which increase the amount of liquid phase in the reaction system and facilitate the carbothermal reduction reaction. More calcium silicate formed in the fly ash fluxing system promotes phosphorus reduction. The fluxing effect by fly ash is stronger and it is more conducive than SiO_2 as a flux to enhance carbothermal reduction of phosphate rock. The results of this paper supply an option to recycle fly ash in green processing and sustainable development.

Acknowledgments: The authors would like to acknowledge the scientific support provided by Wuhan Institute of Technology and National Natural Science Foundation of China (No. 51474160).

Research funding: This research was supported by National Natural Science Foundation of China (No. 51474160).

Author contributions: Jun Ji, Dongsheng He, Qifeng Tian, and Yichang Chen developed the idea of this research and made the problem formulation; Biwei Luo, Pengfei Li, and Yan Li derived the formulas, made the calculations, performed the simulation study, and prepared the initial draft of the paper; Qifeng Tian oversaw all aspects of the research, data analysis, writing, and revised this manuscript. All authors have discussed the results and approved the final version of the paper. All authors have read and agreed to the published version of the manuscript.

Conflict of interest: Authors state no conflict of interest.

References

[1] Kijkowska R, Kowalski Z, Pawlowska-Kozinska D, Wzorek Z, Gorazda K. Tripolyphosphate made from wet-process phosphoric acid with the use of a rotary kiln. Ind Eng Chem Res. 2008;47(18):6821–7.

[2] Lv L, Liang B, Liu Q. Back adsorption process of calcium phosphate to P_2O_5 in kiln phosphoric acid. J Chem Ind Eng. 2016;67(10):4399–405.

[3] Wang X, Tang L, Jiang Z. Numerical simulation of Venturi ejector reactor in yellow phosphorus purification system. Nucl Eng Des. 2014;268(3):18–23.

[4] Chen S. Summary of comprehensive utilization of phosphorus by-products from electric furnace in China. Sulphur Phosphorus Bulk Mater Handl Relat Eng. 2011;5:44–8.

[5] Xue K, Zhang R. Research progress on phosphate resource distribution and metallogenic characteristics in China. Acta Miner Sin. 2019;39(1):7–14.

[6] Kaia T, Kārlis AG, Liene P, Mihkel V. A review on the thermal stability of calcium apatites. J Therm Anal Calorim. 2012;110(2):647–59.

[7] Cheng C, Xue Q, Wang J, Wang G, Zhang Y. Carbothermal reduction mechanism of fluorapatite and gangue in high phosphorus iron ore. J Iron Steel Res Int. 2016;28(4):8–15.

[8] Cao R, Xia J, Li W, Han Y. Effect of alkali metal carbonate on carbothermal reduction of phosphorus rock. J Chem Eng Chin Univ. 2018;32(3):568–76.

[9] Yang J, Chen J, Liu H, Liu D. Process analysis of solid phase carbothermal reduction of fluoroapatite with aluminum impurities. J Sichuan Univ Eng Sci Ed. 2015;47(1):186–91.

[10] Hu B, Ma C, Gui K, Wu Y, Tian Q, Yuan H. Effect of inorganic additives on smelting reduction of phosphate rock. Ind Min Process. 2014;43(6):1–2.

[11] Tang J, Wang D, Hua Q, Liu Y, Liu L. Study on reduction reaction characteristics of phosphate rock by furnace process. Ind Min Process. 2011;40(5):1–3.

[12] Chen Z, Li Y, Xia J. Silica, alkali carbonate and alkali rich metal ore as additive effect on the carbothermic reduction process of phosphorus ore. Silicon. 2020;12:613–20.

[13] Xia J, Geng R, Chen Z. The effect of K-feldspar and silica as fluxing agent on the production process of phosphorus furnace. Silicon. 2019;11:233–9.

[14] Li Y, Chen Z, Geng R, Xia J. Studies on extraction of phosphorus from phosphate ore by electric furnace with different fluxing agents. Phosphorus, Sulfur Silicon Relat Elem. 2018;193:141–8.

[15] Sun W, Liang G. Effect of fluxes on the ash behavior of coal. Coal Convers. 2012;35(2):31–5.

[16] Jin F, Yang Y, Ma C, Zhu X, Wang J, Wu Y. Optimization for conditions of phosphorous production reduced by molten $CaO{\cdot}SiO_2{\cdot}Al_2O_3{\cdot}MgO–P_2O_5$ system. Inorg Chem Ind. 2013;45(11):29–32.

[17] Chen Z, Ma W, Wu J, Wei K, Yang X, Lv G, et al. Influence of carbothermic reduction on submerged arc furnace energy efficiency during silicon production. Energy. 2016;116:687–93.

[18] Chen Z, Ma W, Wei K, Li S, Ding W. Effect of raw materials on the production process of the silicon furnace. J Clean Prod. 2017;158:359–66.

[19] Chen Z, Ma W, Li S, Wu J, Wei K, Yu Z, et al. Influence of carbon material on the production process of different electric arc furnaces. J Clean Prod. 2018;174:17–25.

[20] Huang G, Wang B, Xu H. Research progress on comprehensive utilization and upgrading technologies of fly ash. Conserv Util Miner Resour. 2019;4:32–7.

[21] Guo X. Research on Comprehensive Utilization Technology of Fly Ash in Coal-fired Power Plant [Master Thesis]. Xian, China: Changan University; 2009.
[22] Li X. Study on the process condition and kinetics of low-grade phosphate ore by smelting reduction technology. Master Thesis. Wuhan, China: Wuhan Institute of Technology; 2013.
[23] Hu B, Li X, Hu Y, Jin F, Wu Y. Study on reduction reaction characteristics of phosphate rock by furnace process. Ind Min Process. 2012;12:1–4.
[24] Wang J, Zhang J, Mo F, Mao R, Wu L. Experimental study on selective leaching of medium and low grade phosphorite. Inorg Chem Ind. 2016;48(5):13–5.
[25] Liu J, Liu J, Wu B, Shen S, Yuan G, Peng L. Study on the carbothermal reduction of manganese ore powder in microwave field. J Hunan Univ Nat Sci Ed. 2017;44(12):89–96.
[26] Mu J, Leder F, Park WC, Hard RA, Megy J, Reiss H. Reduction of phosphate ores by carbon: Part I. Process variables for design of rotary kiln system. Metall Mater Trans B. 1986;17(4):861–8.
[27] Qiu L, Liang B, Jiang L. Experimental study on the solid state reduction process of fluorapatite. J Chem Ind Eng. 1996;47(1):65–71.
[28] Sun Y, Li Y, Wang D, Hang Y. Thermodynamic analysis of fluorapatite reduction process. J Northeastern Univ (Nat Sci). 2019;40(6):875–80.
[29] Cao R, Li Y, Xia J, Li W, Han Y. Study on carbothermal reduction process and kinetics of fluoroapatite. J Chem Eng Chin Univ. 2019;33(2):372–9.
[30] Liu Y. Phase Diagrams in Silicate Ceramics, 1st edn. Beijing: Chemical Industry Press; 2011.
[31] Zheng G, Cao R, Li Y, Xia J, Chen Z. The additive effect of K_2CO_3–$NiSO_4$ on the carbothermal reduction process of phosphate rock and SiO_2. Silicon. 2020;(12):1985–94.